

Observations of transient events with Mini-MegaTORTORA wide-field monitoring system with sub-second temporal resolution

S. Karpov^{1,3}, G. Beskin^{1,3}, A. Biryukov^{4,3}, S. Bondar², E. Ivanov²,
E. Katkova², N. Orekhova², A. Perkov² and V. Sasyuk³

¹ *Special Astrophysical Observatory of Russian Academy of Sciences,
Nizhniy Arkhyz 369167, Russia*

² *Open Joint-stock Company “Research-and-Production Corporation Precision
Systems and Instruments”, “Arkhyz” Optical Observation Station,
Nizhniy Arkhyz 369167, Russia*

³ *Kazan Federal University,
16a Kremlyovskaya St., Kazan 420008, Russia*

⁴ *Moscow State University,
13 Universitetskii pr., Moscow 119234, Russia*

Received: May 11, 2017; Accepted: May 21, 2017

Abstract. Here we present the summary of first years of operation and the first results of a novel 9-channel wide-field optical monitoring system with sub-second temporal resolution, Mini-MegaTORTORA (MMT-9), which is in operation now at Special Astrophysical Observatory on Russian Caucasus. The system is able to observe the sky simultaneously in either wide (900 square degrees) or narrow (100 square degrees) fields of view, either in clear light or with any combination of color (Johnson-Cousins B, V or R) and polarimetric filters installed, with exposure times ranging from 0.1 s to hundreds of seconds. The real-time system data analysis pipeline performs automatic detection of rapid transient events, both near-Earth and extragalactic. The objects routinely detected by MMT also include faint meteors and artificial satellites.

Key words: Instrumentation: photometers – Instrumentation: polarimeters – Techniques: high temporal resolution

1. Introduction

Mini-MegaTORTORA is a novel robotic instrument developed according to the principles of MegaTORTORA multi-channel and transforming design formulated by us earlier (Beskin et al., 2010a; Biryukov et al., 2015) in order to detect and characterize fast optical transients of various origins, both cosmological, galactic and near-Earth. The importance of such instruments became evident after the discovery and detailed study of the brightest ever optical afterglow of a gamma-ray burst, GRB 080319B (Racusin et al., 2008; Beskin et al., 2010b).

Mini-MegaTORTORA is a 9-channel wide-field (~ 900 square degrees) monitoring system with temporal resolution down to 0.1 seconds and limit down to $V \sim 11$ mag on this time scale. Every channel of Mini-MegaTORTORA has 10×10 deg field of view and is equipped with installable photometric and polarimetric filters and coelostat mirror for a rapid repointing in a limited range (± 15 degrees). It allows to re-configure the system on the fly from wide-field to narrow-field regime in order to rapidly follow-up the transients just detected.

2. Mini-MegaTORTORA operation

Mini-MegaTORTORA started its operation in Jun 2014, and routinely monitor the sky since then. The observations are governed by the dedicated dynamic scheduler optimized for performing the uniform sky survey every night. The scheduler works by selecting the next pointing for Mini-MegaTORTORA by simultaneously optimizing the following parameters: distances from the Sun, Moon and the horizon should be maximized, distances from the current pointings of Swift and Fermi satellites should be minimized, and the number of frames already acquired on a given sky position that night should be minimized. In this way more or less uniform survey of the whole sky hemisphere is being performed while maximizing the probability of observations of gamma-ray bursts. As an un-optimized extension, the scheduler also supports the observations of pre-selected targets given by their coordinates, which may be performed in various regimes supported by Mini-MegaTORTORA (wide-field monitoring of a given region of the sky with or without filters, narrow-field multicolor imaging or polarimetry with lower temporal resolution, etc).

2.1. Real-time transient detection

The main regime of Mini-MegaTORTORA operation is the wide-field monitoring with high temporal resolution and with no photometric filters installed. In this regime, every channel acquires 10 frames per second, which corresponds to 110 megabytes of data per second. To analyze it, we implemented the real-time fast differential imaging pipeline intended for the detection of rapidly varying or moving transient objects – flashes, meteor trails, satellite passes etc. It is analogous to the pipeline of FAVOR and TORTORA cameras (Beskin et al., 2004; Karpov et al., 2010), and is based on building an iteratively-updated comparison image of current field of view using numerically efficient running median algorithm, as well as threshold image using running similarly constructed *median absolute deviation* estimate, and then comparison of every new frame with them, extracting candidate transient objects and analyzing lists of these objects from the consecutive frames. It then filters out noise events, extracts the meteor trails by their generally elongated shape on a single frame, collects the events corresponding to moving objects into focal plane trajectories, etc. Data

on detected transients are stored to the database and are partially published online¹.

Every 100 frames acquired by a channel are being summed together, yielding “average” frames with 10 s effective exposure and better detection limit. Using these frames, the astrometric calibration is being performed using locally installed `ASTROMETRY.NET` code by Lang *et al.* (2010). Also the rough photometric calibration is being done. These calibrations, updated every 10 seconds, are used for measuring the positions and magnitudes of transients detected by the real-time differential imaging pipeline. The “average” frames are stored permanently (in contrast to “raw” full-resolution data which is typically erased in a day or two after acquisition) and may be used later for studying the variability on time scales longer than 10 s.

The Mini-MegaTORTORA typically observes every sky field continuously for a 10000 seconds before moving to the next pointing. Before and after observing the field with high temporal resolution, the system acquires deeper “survey” images with 60 seconds exposure in white light in order to study the variability of objects down to 14-15 magnitude on even longer time scales; typically, every point of the northern sky is covered by one or more such images every observational night.

Mini-MegaTORTORA real-time transient detection system routinely extracts various kinds of transient from the data stream – rapid flashes, meteors, satellites etc.

The rapid flashes – i.e. the optical transients rapidly changing their brightness and not displaying signs of motion – are then matched against stellar catalogues to exclude events due to stellar scintillations, and against public NORAD database of satellite orbits to filter out satellite flashes. All the remaining flashes have the same characteristic properties – durations, shapes, peak magnitudes (see Figure 2) – as the ones caused by identified satellites, and we may suggest that they are also due to satellites, but either missing from public database of orbits, or having quite large errors in their orbital parameters. Moreover, immediate follow-up observations using Mini-MegaTORTORA rapid reaction mode (see Figure 1 for a typical example) often reveal faint satellite trails leading from the event location. Therefore we may conclude that no bright rapid flashes of astrophysical origin are detected in 2.5 years of Mini-MegaTORTORA operation.

2.2. Follow-up observations of external triggers

Mini-MegaTORTORA also performs follow-up of Swift, Fermi and LIGO-Virgo triggers. Its large field of view, allowing for simultaneous observations of ~ 900 sq.deg. sky regions, makes it the perfect instrument for following up events with

¹Public databases of meteors (Karpov *et al.*, 2016c) and artificial satellites (Karpov *et al.*, 2016b) observed by Mini-MegaTORTORA are available at project website at <http://mmt.favor2.info>

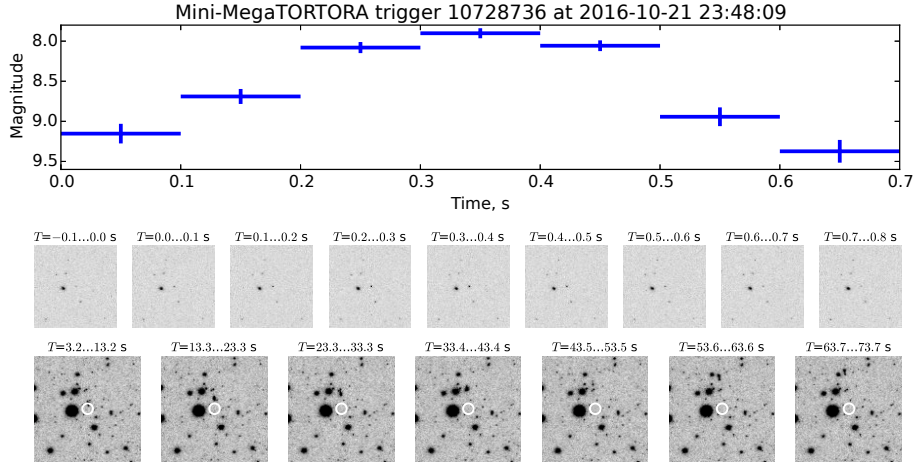


Figure 1. Example of a rapid optical flash independently detected and followed-up by Mini-MegaTORTORA and not identified with satellites from NORAD database. Upper panel – light curve with 0.1 s temporal resolution, middle panel – corresponding detection images ($50' \times 50'$ around the event), lower panel – follow-up images with 10 s exposures that clearly reveal a satellite slowly moving away from the flash position.

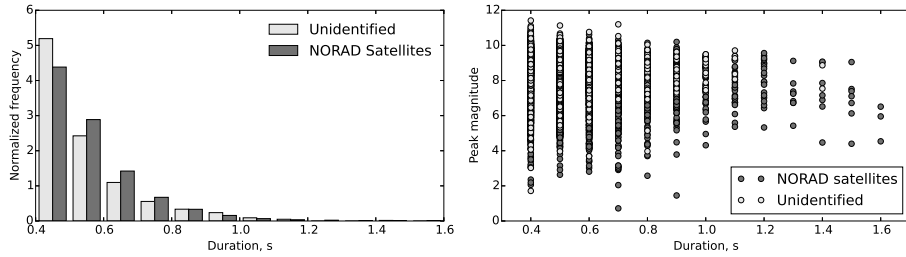


Figure 2. Comparison of durations (left panel) and brightness (right panel) of rapid flashes detected by Mini-MegaTORTORA and identified/non-identified with NORAD satellites.

poor localization accuracy. On the other hand, the triggers with better localizations may be observed in multicolor and/or polarimetric regimes simultaneously.

Since mid-2015, 4 of 89 Swift GRBs have been followed up in narrow-field polarimetric mode in 30 to 60 seconds since trigger distribution through GCN network, with no optical emission detections. 9 of 250 Fermi GBM triggers have been also followed up in wide-field mode in 20 to 90 seconds from the trigger. All other events were either below the horizon or occurred in bad weather conditions.

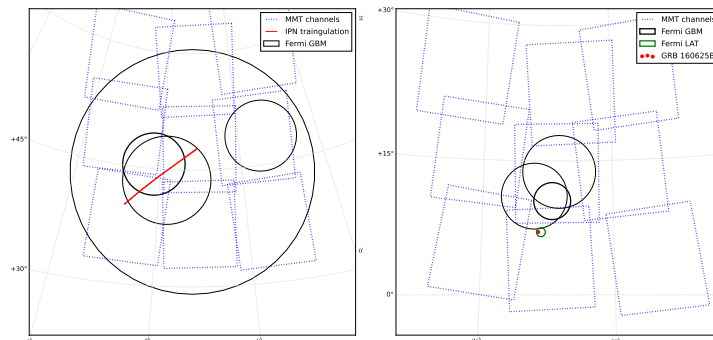


Figure 3. Left – the gradual improvement of GBM localization of GRB 151107B over time, and the Mini-MegaTORTORA field of view at the moment of its trigger (9 channels in wide-field regime). Most of final GBM localization, as well as IPN triangulation error box, was inside Mini-MegaTORTORA field of view. Right – the same for GRB 160625B, with smallest circle representing final LAT error box, and the dot – the localization of optical transient, well outside original 1-sigma circle used for the Mini-MegaTORTORA follow-up (9 channels in wide-field regime).

2.3. Simultaneous observations of Fermi GRB 151107B

The localization of Fermi GBM trigger GRB 151107B (Stanbro & Meegan, 2015; Karpov et al., 2015) has been observed before, during and just after the trigger time, covering nearly all its error box (see Figure 3) simultaneously since $T - 329.3$ s till $T + 25.7$ (including brightest part of first gamma-ray peak) with temporal resolution of 0.1 s in white light. Dedicated real-time transient detection pipeline did not detect any events longer than 0.3 s and brighter than approximately $V = 10.5$ mag. Inspection of co-added images with 10 s effective exposure has not revealed any variable source down to $V = 12.0$ mag during that interval.

After receiving GCN trigger the system initiated a wide-field follow-up and since $T+62.7$ s (during the continuing gamma-ray activity) till $T + 666.7$ s acquired 20×9 deep images with 30 s exposures in a 30×30 degree field of view covering the whole final 1-sigma localization box. Analysis of the acquired data has not revealed any variable object down to roughly $V = 13.5$ mag over the time interval (Karpov et al., 2015).

3. Detection of the optical counterpart of Fermi GRB 160625B

One more Fermi event, GRB 160625B, has been followed up in the widefield regime, with bright optical flash of GRB 160625B clearly detected during the

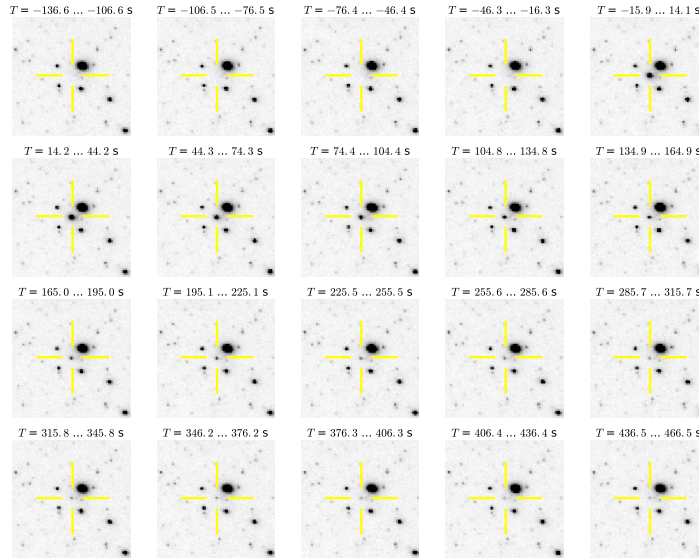


Figure 4. The final localization region of GRB 160625B as seen by Mini-MegaTORTORA (20 unfiltered images with 30-s exposures). The peak brightness of transient object is $V=8.8$ mag.

gamma activity (Karpov et al., 2016a).

The on-sky position of the Fermi gamma-ray burst GRB 160625B has been observed before, during and just after the LAT trigger time ($T = 2016-06-25$ 22:43:24). Mini-MegaTORTORA reacted to the Fermi GBM trigger no. 488587220 generated as a result of the detection of the precursor and started observing its error box 52 seconds after it and 136 seconds before LAT trigger. Due to large size of GBM error box, the observations have been performed in “widefield+deep” regime, with channels simultaneously covering 30×30 deg field of view (see Figure 3) with 30 s exposures in white light to achieve deepest detection limit. The system acquired 20 frames in such regime, covering time interval from $T - 136$ to $T + 466$ s, and detected a bright optical transient with a magnitude of about $V = 8.8$ mag on a frame coincident with LAT trigger time ($T - 15.9 - T + 14.1$ s) at the coordinates consistent with the afterglow (Troja et al., 2016). On the consecutive frames, the transient brightened for about 0.1 mag, and then faded following nearly smooth power-law decay with slope of about -1.6 , down to $V = 12.2$ at last acquired frame. The images acquired prior to LAT trigger do not display any object at that position down to about $V = 13.5$ mag. This sequence of frames (20’ subimages centered on the transient) is shown in Figure 4.

The system also responded to the second GBM trigger no. 488587880 with

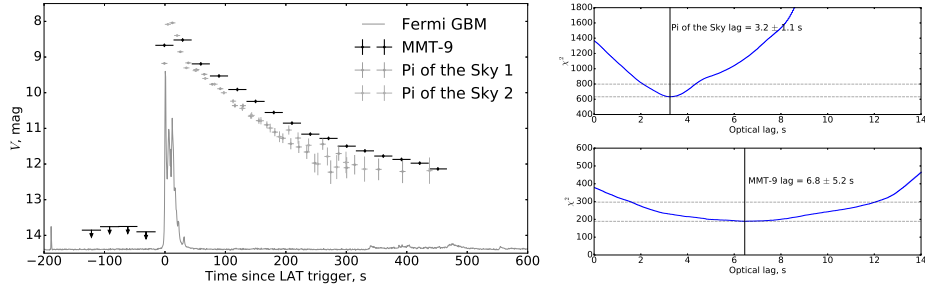


Figure 5. Left – the light curve of optical transient that accompanied the second gamma activity episode of GRB 160625B, as seen by Mini-MegaTORTORA. Also, the data acquired by Pi of the Sky cameras (Batsch et al., 2016) are shown. Right – The determination of a lag between optical and gamma ray light curves of GRB 160625B, using optical measurements from Mini-MegaTORTORA and Pi of the Sky.

a somewhat different coordinates. This response resulted in the acquisition of 20 more frames covering burst position in the time interval from $T + 1691$ to $T + 2264$ s. In this sample no transient objects brighter than $V = 13.5$ mag were detected.

The optical light curve shown in Figure 5 displays an initial peak with duration similar to the one of the gamma-ray peak and seemingly corresponding to the prompt phase of emission, gradually transforming into the afterglow about 50 s after the onset of the gamma-ray event. Such a behavior – the absence of the intensity dip between the prompt optical emission accompanying the gamma-ray burst and the afterglow – is typical for several most powerful bursts including GRB 080319B (Naked-Eye Burst) (Beskin et al., 2015). This is not the only similarity between these two events. Indeed, in both cases the intensity of the optical emission accompanying the gamma-ray burst exceeds the extrapolation of the gamma-ray spectrum to the optical range, which indicates different generation mechanisms of these two emission components. Moreover, gamma-ray peaks precede the corresponding optical flashes in time. Indeed, a comparison of the light curves of GRB 160625B in different spectral intervals (see Figure 5 where we used both the Mini-MegaTORTORA data and the results obtained by Pi of the Sky wide-field monitoring system (Batsch et al., 2016)) shows that optical and gamma-ray emission in the second activity episode are correlated, and the latter precedes the optical flash by 2–4 s. Given the measured redshift of the object, which was found to be close to 1.4 (Xu et al., 2016), we find that in the comoving frame optical emission lags behind gamma-ray emission for 1–2 s, like in the Naked-Eye Burst where the same lag was found. We may conclude that in both cases optical photons are born 10–100 times farther away from the “central engine” than high-energy photons, i.e., in jet regions that are spaced

apart (Beskin et al., 2010b), and that in the GRB 160625B electrons are heated by internal shocks originating from the residual collisions of filaments ejected in the jet, and the observed emission is generated by their synchrotron energy release (Li & Waxman, 2008).

Acknowledgements. Mini-MegaTORTORA belongs to Kazan Federal University and the work is performed according to the Russian Government Program of Competitive Growth of Kazan Federal University. Observations on Mini-MegaTORTORA are supported by the Russian Science Foundation grant No. 14-50-00043. The reported study was funded by RFBR according to the research project No. 17-52-45048.

References

- Batsch, T., Castro-Tirado, A. J., Czyrkowski, H., et al. 2016, *GRB Coordinates Network*, **19615**
- Beskin, G., Biryukov, A., Bondar, S., et al. 2004, *Astronomische Nachrichten*, **325**, 676
- Beskin, G., Bondar, S., Karpov, S., et al. 2010a, *Advances in Astronomy*, **2010**
- Beskin, G., Karpov, S., Bondar, S., et al. 2010b, *ApJ*, **719**, L10
- Beskin, G. M., Oganessian, G., Greco, G., & Karpov, S. 2015, *Astrophysical Bulletin*, **70**, 400
- Biryukov, A., Beskin, G., Karpov, S., et al. 2015, *Baltic Astronomy*, **24**, 100
- Karpov, S., Beskin, G., Bondar, S., et al. 2010, *Advances in Astronomy*, **2010**
- Karpov, S., Beskin, G., Bondar, S., et al. 2016a, *GRB Coordinates Network*, **19603**
- Karpov, S., Beskin, G., Bondar, S., et al. 2015, *GRB Coordinates Network*, **18574**
- Karpov, S., Katkova, E., Beskin, G., et al. 2016b, in *Revista Mexicana de Astronomia y Astrofisica Conference Series*, Vol. 48, *Revista Mexicana de Astronomia y Astrofisica Conference Series*, 112–113
- Karpov, S., Orekhova, N., Beskin, G., et al. 2016c, in *Revista Mexicana de Astronomia y Astrofisica Conference Series*, Vol. 48, *Revista Mexicana de Astronomia y Astrofisica Conference Series*, 97–98
- Lang, D., Hogg, D. W., Mierle, K., Blanton, M., & Roweis, S. 2010, *Astron. J.*, **139**, 1782
- Li, Z. & Waxman, E. 2008, *ApJ*, **674**, 65
- Racusin, J. L., Gehrels, N., Holland, S. T., et al. 2008, *GRB Coordinates Network Circular*, **7427**, 1
- Stanbro, M. & Meegan, C. 2015, *GRB Coordinates Network*, **18570**
- Troja, E., Butler, N., Watson, A. M., et al. 2016, *GRB Coordinates Network*, **19588**
- Xu, D., Malesani, D., Fynbo, J. P. U., et al. 2016, *GRB Coordinates Network*, **19600**